A Simplified Numerical Model for Simulating Sliding Door and Surgical Staff Movement in an Operating Theatre

C.Balocco[1]
[1] Department of Energy Engineering, “Sergio Stecco”, University of Firenze
*Corresponding author: via Santa Marta 3 50139 Firenze (Italy), carla.balocco@unifi.it

Abstract: This paper deals with a numerical investigation on sliding door and people moving effects on the indoor climate of a standard ISO5 class OT with an ultraclean air filter system and a total ceiling unidirectional diffuser. A simple method to analyze the effects on the OT climate by different sliding door conditions combined with crossing persons and persons with a stretcher crossing is provided.

The proposed procedure consists in defining some user-defined logical functions in COMSOL Multiphysics models. Results, obtained for different typical cases, show a strong influence of the surgery staff movements and sliding door opening/closing on the internal flow patterns and in static pressure variation inside the OT also. These effects are related to the operating conditions of HVAC plant system, allowing to carry-out important predictions on the effects on ventilation system working conditions. Our proposed method indicates the opportunity of simulating the influence of objects movement in a fluid -filled space using a relatively simple CFD model.

Keywords: Operating Theatre, ventilation, Indoor Air Quality, sliding doors, CFD-FEM simulation.

1. Introduction

In recent years several studies have focused on computational models using fluid dynamics approaches to investigated airflow patterns and the related spreading of infection in isolation and hospitalization rooms and in particular in OTs for different ventilation systems (for example operating under open or closed-door conditions) [12]. A recent article [4] shows the contamination diffusion in an ISO5 class operating room with vertical LAF when the door is open by a computational fluid dynamic (CFD) simulation. In this last paper, the influence of the door-opening procedure was ignored since the door of the operating room is a sliding one and in particular the effect of people crossing with and without a stretcher is disregarded.

Some authors used numerical [2,11] or experimental [8] approaches to investigate the effects of one moving person or sliding doors on the air distribution, including air velocity and pressure field but also CO_2 contaminant distribution, within generic ventilated or specific negative pressure isolation room [5]. Simulation of object or person movements has been handled directly or indirectly. Direct simulation includes the real movement of the real “object” inside the solution domain and requires a moving mesh approach in order to be realized. One of the most recent methods used for this kind of application is the so-called Arbitrary Lagrangian-Eulerian (ALE) method, in certain cases allowing resolution of the limit of small distortions allowed in the numerical model by the traditional Lagrangian approach. However, the direct simulation of the moving object requires very expensive computational cost. They are related on the one hand to the degrees of freedom increasing for a chosen number on mesh nodes, and on the other to the re-meshing procedure, often needed during computations. The basic principle of the indirect simulation of a moving object in surrounding air consists otherwise in keeping into account the effects of the object’s movement on the air flow. Two indirect numerical procedures were recently tested and applied by [2] to simulate the effect of the surgical staff movements on contaminant concentration in an operating room.

Starting from these important recent research and literature evidence in the present paper an ISO5 class OT climate changing due to different sliding doors conditions and surgical staff crossing was investigated. This work belongs to a wide research on this topic and then to a recent published paper [1]. Here the simple method used to analyze the effects of different sliding door conditions combined with crossing persons and persons with a stretcher crossing, on the climate, airflow patterns and indoor pressure scheme on a standard ISO5 class OT, with a vertical LAF [1], is highlighted and widely explained. Our method can be used for the comprehension and analysis of the airflow and pressure distribution in the entire operating theatre space and then of the HVAC working conditions imposed by important pressure variations.

2. The solid model of the standard ISO5

The physical and architectural 3D model of the OT used in the present study was based on a typical and standard layout of the ISO5 class with ultra clean air filters system. The operating room is 6.3 m wide, 6.3 m long with a total volume of 119.07 m^3. All the internal partition walls have a thermal transmittance of 2.33 $W/(m^2K)$. The HVAC plant systems meets the standard requirements: its functional and operating parameters of the plant system with primary air unit and a ceiling unidirectional diffuser are provided in Tab. 1. The sliding door clear opening of the O.T. is 900 mm x 2100 mm with a thickness of 40 mm, representative of a door made by an aluminium frame and a galvanized steel sheet panel with a finished powder coating.

Tab.1 Air ceiling unidirectional inlet diffuser parameters.

Effective surface (>90% of floor area)	36 m^2
ACH (Air Change per Hour)	200 1/h
Min air change flow rate	1500 m^3/h
ventilation air flow rate	23814 m^3/h
Recirculation air flow rate	22314 m^3/h
Mean inlet velocity	0.184 m/s
Minimum over-pressure differential	5 Pa

The internal air temperature of the OT was set at 20 °C and that of all the surrounding zones (T_{ext}) is assumed at 26 °C as suggested. Dimension and design parameters of the air extraction grids are reported in Tab.2.

Tab. II: Air recovery grids parameters.

Total number of diffusers	8 [-]
Width	0.35 [m]
Length	0.6 [m]
Effective surface	0.21 [m^2]
Total extraction area	1.68 [m^2]
Mean outlet velocity	3.94 [m/s]

Physical properties assumed for fluid, walls and solid are provided in Tab.3. Furniture, basic safety lighting systems, surgical lighting surgical staff position were disregarded but thermal power provided were considered: the total thermal power released by 8 persons was taken a 920 W, for general lighting 400 W and for surgical equipment 1 kW; metabolic rate was assumed 2Met (walking), that corresponds to a specific heat source of 1300 W/m^3.

Tab. III Physical properties adopted.

	S.I Unit	"Fluid"	"Solid"	Wall
ρ	[kg/m^3]	1.2	900	600
ρ	[Pa s]	5E-5	1E+5	-
k	[W/(m K)]	0.62	0.6	0.16
C_p	[J/(kg K)]	1004	2000	840

The geometry of the studied system is outlined in Fig. 1: the OT is accessible from a 3 m breadth adjacent corridor by a two-panels sliding door, represented in blue. Its geometrical symmetry with respect to the mid *ZX*-plane, allows to consider one half of the studied system for computations. This assumption was validated by some preliminary tests that were carried-out by considering the full geometry of the system.

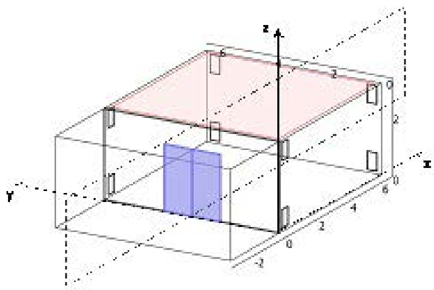

Figure 1 The O.T. geometry and the "zx" symmetry plane (dashed lines) considered for studying of one half of the model.

3. Numerical model and transient simulations

Modelling of solid objects moving is handled by an indirect method, that mainly consists in keeping into account the effects of the object's movement on the airflow without simulating the real solid objects movements in inside the numerical domains, that requires a moving mesh approach in order to be realized.

Those functions assume binary values that identify the portions of domain where solid objects are located (binary value 1) or not (binary value 0) at the initial time of the transient simulation. The binary value assumed by the logical functions depends on assigned geometrical coordinates for each object. In those regions fluid-dynamical properties and source terms assume specific values, defining the fluid conditions. Time-dependent functions allow modification of the geometrical coordinates identifying the position of the “solid” objects during time, so that a prescribed motion law can be assigned to the moving objects. The adopted procedure is mainly based on the definition of specific source terms in the governing equations, with assigned values in the portions of the computational domains where the solid objects are located at a chosen time. Moving of interfaces describing the position of the solid object, that are not explicitly designed in the geometrical models, is driven by some logical functions preliminarily defined, that allow simulating of the dynamics associated with the sliding door opening/closing and persons walking across the OT. To investigate the turbulent air flow inside the OT, the Reynolds Averaged Navier-Stokes and energy equations were numerically solved under the assumption of Newtonian fluid and uncompressible flow.

Momentum equations are coupled with a standard k-ε closure scheme [6,7], applied in order to model turbulence by an eddy viscosity approach. Continuous equations used are as following:

$$\rho\frac{\partial \mathbf{U}}{\partial t}+\rho(\mathbf{U}\cdot\nabla)\mathbf{U}=\nabla\cdot\left[-p\mathbf{I}+(\mu+\mu_T)\left(\nabla\mathbf{U}+(\nabla\mathbf{U})^{\mathrm{T}}\right)\right]+F_{dom} \qquad (1)$$

$$\nabla\cdot\mathbf{U}=0 \qquad (2)$$

$$\rho\frac{\partial k}{\partial t}+\rho\mathbf{U}\cdot\nabla k=\nabla\cdot\left[\left(\mu+\frac{\mu_T}{\sigma_k}\right)\nabla k\right]+\frac{1}{2}\mu_T\left[\nabla\mathbf{U}+(\nabla\mathbf{U})^{\mathrm{T}}\right]^2-\rho\varepsilon \qquad (3)$$

$$\rho\frac{\partial \varepsilon}{\partial t}+\rho\mathbf{U}\cdot\nabla \varepsilon=\nabla\cdot\left[\left(\mu+\frac{\mu_T}{\sigma_\varepsilon}\right)\nabla \varepsilon\right]+\frac{1}{2}C_{\varepsilon 1}\frac{\varepsilon}{k}\mu_T\left[\nabla\mathbf{U}+(\nabla\mathbf{U})^{\mathrm{T}}\right]^2-\rho C_{\varepsilon 2}\frac{\varepsilon^2}{k} \qquad (4)$$

$$\rho C_p\frac{\partial T}{\partial t}+\rho C_p\mathbf{U}\cdot\nabla T=\nabla\cdot(\lambda\nabla T)+Q_{dom} \qquad (5)$$

Where $\mu_T = \rho C_\mu k^2/\varepsilon$ represents the turbulent viscosity. Values adopted for constants appearing in the above equations are determined from experimental data [13] and reported in Tab. IV. Boundary conditions considered for the model are in Tab. V. Logarithmic wall functions were applied in the near wall flow, that has been considered parallel to the wall and being in a wall offset δ_w equal to one half of the boundary mesh element dimension. The equivalent wall offset in viscous unit is defined as $\delta_w^+ = \delta_w \rho U_\tau / \mu$, U_τ the frictional velocity.

Tab. IV Numerical values of constants appearing in the adopted mathematical model.

C_μ	$C_{\varepsilon 1}$	$C_{\varepsilon 2}$	σ_k	σ_ε
0.09	1.44	1.92	1.0	1.3

Tab. V Expression of applied boundary conditions.

Eq.	Boundary condition	
(1-2)	Inlet	Symmetry
	$\mathbf{U}=-U_{in}\mathbf{n}$	$\mathbf{n}\cdot\mathbf{U}=0$ $\mathbf{t}\cdot\left[-p\mathbf{I}+(\mu+\mu_T)\left(\nabla\mathbf{U}+(\nabla\mathbf{U})^{\mathrm{T}}\right)\right]\mathbf{n}=0$
	Output	Open
	$\left[(\mu+\mu_T)\left(\nabla\mathbf{U}+(\nabla\mathbf{U})^{\mathrm{T}}\right)\right]\mathbf{n}=0$ $p=p_{out}$	$\left[-p\mathbf{I}+(\mu+\mu_T)\left(\nabla\mathbf{U}+(\nabla\mathbf{U})^{\mathrm{T}}\right)\right]\mathbf{n}=0$
	Wall	
	$\mathbf{n}\cdot\mathbf{U}=0$ $\left[(\mu+\mu_T)\left(\nabla\mathbf{U}+(\nabla\mathbf{U})^{\mathrm{T}}\right)\right]\mathbf{n}=\left[\rho C_\mu^{0.25}k^{0.5}/\left(\ln\left(\delta_w^+\right)/\kappa+C^+\right)\right]\mathbf{U}$	
(3)	Inlet	Symmetry
	$k=3/2\left(I_T U_{in}\right)^2$	$\mathbf{n}\cdot\left[(\mu+\mu_k/\sigma_k)\nabla k-\rho\mathbf{U}k\right]=0$
	Output / Open	Wall
	$\mathbf{n}\cdot\nabla k=0$	$\mathbf{n}\cdot\nabla k=0$
(4)	Inlet	Symmetry
	$\varepsilon=C_\mu^{0.75}\left(3/2\left(I_T U_{in}\right)^2\right)^{1.5}/L_T$	$\mathbf{n}\cdot\left[(\mu+\mu_T/\sigma_\varepsilon)\nabla\varepsilon-\rho\mathbf{U}\varepsilon\right]=0$
	Output / Open	Wall
	$\mathbf{n}\cdot\nabla\varepsilon=0$	$\varepsilon=\rho C_\mu k^2/\left(\kappa\delta_w^+\mu\right)$
(5)	Inlet	Symmetry / Insulation
	$T=T_{in}$	$\mathbf{n}\cdot(\lambda\nabla T)=0$
	Output	Dispersion
	$\mathbf{n}\cdot(\lambda\nabla T)=0$	$\mathbf{n}\cdot(\lambda\nabla T)=h_{conv}\left(T_{ext}-T\right)$

Assumed values for the constant C^+ is 5.5, while the Karman’s constant value was set equal to 0.42. Under the assumption of fully turbulent flow ($\mathrm{Re}\approx 1.5E+4$), a turbulent length scale of 0.01 m and a 5% of turbulent intensity were applied at the air inlet section. The specific meaning of the source terms appearing in equations (1-5) and their analytical expression are reported in the Appendix, as well as the time-spatial-dependent values adopted for physical properties in the numerical domains. The procedure mainly consists in defining some logical functions assuming binary values that identify the portions of domain where solid objects are located (binary value 1) or not (binary value 0) at the initial time. The binary value assumed by the logical functions depends on assigned geometrical coordinates for each object. In those regions fluid-dynamical properties and source terms assume specific values determining rest conditions for fluid.

Time-dependent functions allow modification of the geometrical coordinates identifying the position of the “solid” objects during time, so that a prescribed motion law can be assigned to the moving objects. Continuous equations were spatially discretized by FEM based on the Galerkin method on non-uniform and non-structured computational grids made of tetrahedral Lagrange second order elements. Influence of spatial discretization was studied to assure mesh-independent results: then mesh of 250000 elements was used for transient simulations. To prevent rising and propagation of numerical instabilities, an artificial streamline diffusion technique, based on the Galerkin Least-Squared (GLS) method, was employed. PARDISO direct solver particularly efficient in order to solve unsymmetrical sparse matrixes by a LU decomposition technique, was used. Computations were carried-out on a workstation disposing of two 64-bit quad-core processors speeding up to 3GHz of frequency and handling 32GB of RAM. Simulations were performed for three cases:

1. Opening and closing of the sliding door (Case A);
2. Opening of the sliding door, one person crossing, closing of the sliding door (Case B);
3. Opening of the sliding door, two persons with a stretcher crossing, closing of the sliding door (Case C).

Validation of the adopted numerical scheme was preliminary performed in order to check the reliability of the provided numerical results.

4. Results and Discussion

Steady solutions of the system, that were mainly carried-out to be used as initialisation state for transient simulations, were performed taking into account the closed sliding door and the person/s and stretcher standing in front of the door on the corridor side. Analyzing the steady air velocity distribution (Fig.2), the efficiency of the ventilation system is particularly evident: in the central zone of the OT, usually occupied by the surgical bed and staff, the plant guarantees appropriate conditions in terms of flow pattern and air velocity magnitude. The flow is almost unidirectional, from the ceiling to the ground, highlighting the total absence of any recirculation zone and turbulence air distribution all over the room volume. The air distribution and assessment of ventilation effectiveness, a good agreement between simulation results and literature can also be deduced [9,3,10]. The velocity field simulated magnitude respects the indoor limits suggested as admissible by the most important standards (0.15-0.2 m/s). In addition, at closed door conditions, the average air pressure inside the OT remains stable and uniform and at the same time, the over-pressure value in regard to the anti-room respects the standard limits of 15-20 Pa, as illustrated in Fig. 3. Fig. 4 shows the temperature distribution field is very uniform in the whole air volume and its mean value is 20 °C as standards suggested. In the zone of the partition wall facing the corridor, the isothermal line distribution highlights the local heat flux.

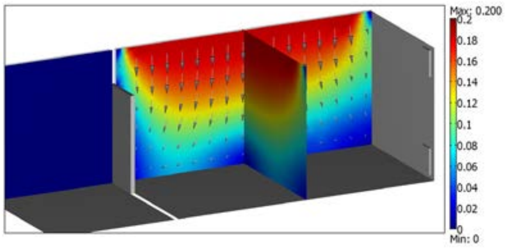

Figure 2 Steady velocity [m/s] and velocity vectors in vertical sections.

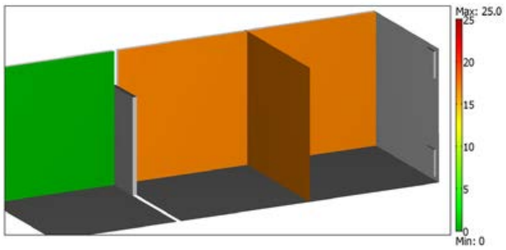

Figure 3 Steady pressure [Pa] in vertical sections.

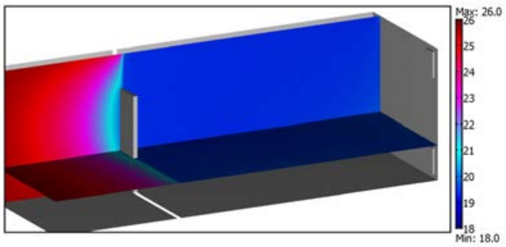

Figure 4 Temperature [°C] in vertical and horizontal sections.

Fig. 5 shows the velocity field and the velocity vectors in a horizontal slice of the OT (1.5 meters from the floor) during the door opening in the Case A. Due to the pressure level inside the OT, a flow rate of air from the room to the corridor is highlighted when the door opens. The maximum magnitude of the flow velocity is reached for a partial opening position of the door. Simulation results show the air distribution that is significantly perturbed by the persons/stretcher incoming inside the OT, that involves in local air-stream from the OT to the corridor, reaching values of velocity magnitude up to 1.5 m/s.

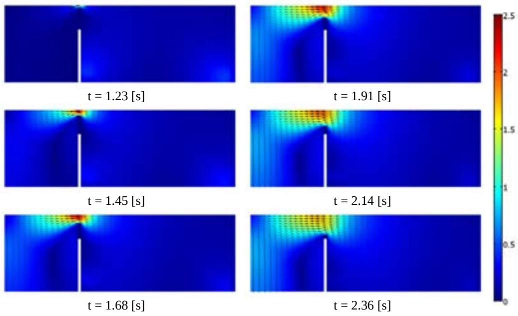

Figure 5 Velocity field [m/s], velocity vectors in horizontal plane (*z* = 1.5) at several time instants during the door opening (Case A).

For the three cases studied A,B,C the effect of the door opening on the pressure levels inside the OT were estimated. Obtained results for the three cases studied highlight that pressure variation due to the door opening are important and in particular cause a pressure reduction from 17 Pa to 4 Pa, that represents the limit imposed by the most restrictive standards. In all the cases studied (A,B,C) the pressure trend, that was evaluated in the middle of the room at 1 m from the floor, is very similar (Fig 6, not-filled symbols). The pressure variations were also evaluated in the plane section of the door, for the three cases during the opening condition, at 1 m from the floor (Fig. 6, filled symbols). The obtained results are similar for all the cases studied except for the case A, for which the over-pressure value with respect to the adjacent corridor one reaches the minimum of 1.12 Pa. The air flow rate crossing the door was also computed during the transient analyses in the three case studies. Time evolutions of the air flow rate (Fig.7) show different behaviour for the cases studied. As a matter of fact, for case A (continuous line), when the door is opening, the air flow rate outgoing increases and spreads to the border of the open door. Then it decreases together with the door closing. For case B, when the door is opening, the air flow rate goes outside the room.

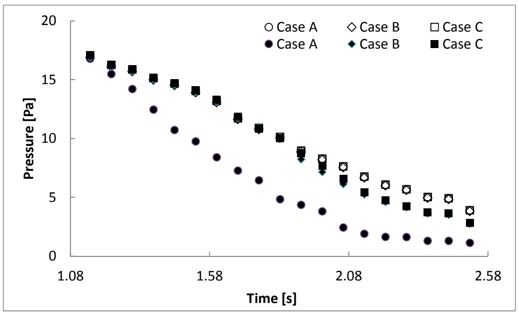

Figure 6 Time evolution of pressure during the door opening for the three case studies.

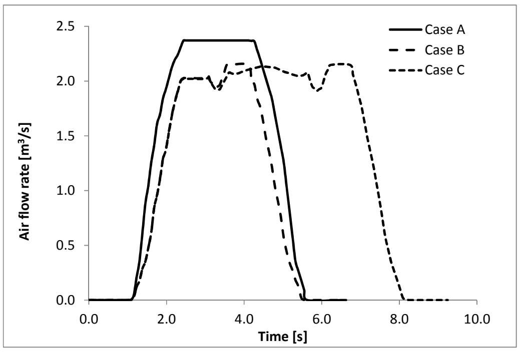

Figure 7 Time evolution of air flow rate throughout the door-space for the three case studies.

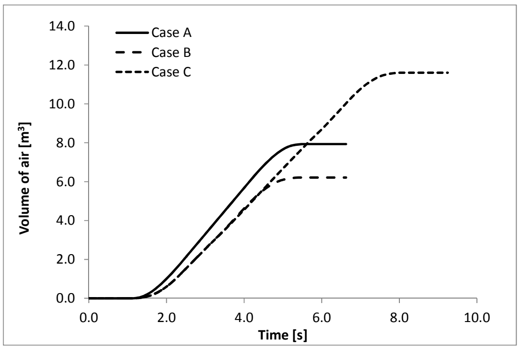

Figure 8 Total volume of air outgoing the OT during the transient analyses for the 3 studied cases

The curve slope (dashed line) is lower compared with case A, because person presence is a real obstacle to the outgoing of the air flow. Two "plateau" zones can then be remarked, spaced by an remarkable decrease of the air flow rate when the person is crossing the clear space. In case C, two "plateau" zones are also detectable from Fig. 7 (dotted line) and spaced by two air flow rate decreasing events, coherently related to the two persons crossing the clear space. In addition, an intermediate zone characterized by the air flow rate increasing-decreasing events is present, that identifies the stretcher crossing of the clear space. The total air volume outgoing from the room to the corridor was also calculated, during transient conditions for all three cases studied, by a discrete time-integration in post-processing of the air flow rate during time (Fig. 8). This provided a validation of the obtained results compared to those expected. The opening and closing of the sliding door more strongly affects the internal over-pressure condition and air velocity distributions, rather than person and/or persons with stretcher crossing.

5. Conclusions

Transient numerical simulations were performed to assess the effect of sliding doors and staff movements on the climate conditions in an ISO5 class OT. Our study provides a simplified indirect numerical method to simulate the influence of solid objects movement, that exploits analytical expressions to dynamically track the solid-fluid interfaces in the computational domain. Special source terms were implemented in the governing equations in order to enable air-flow in domain's portions where solid objects are located at a chosen time. The used turbulence method was preliminary validated by comparing numerical results with experimental data available in literature for similar cases. Other literature evidences were compared to our main findings. Results, obtained for the three cases studied, highlight a strong modification of the air velocity field inside the OT, due to sliding door and staff movements. Air leakages through the door clear-space were estimated for each configuration. The introduction of the practice of performing CFD transient simulation on real cases could be an effective, low cost, means of prediction and control. The provided simulation method can yield significant findings and recommendations for the OT design. The proposed method contributes to showing that CFD-FEM simulations can provide a basic support for the issues involved in analysis and preventive studies of surgical site infection risk.

5. Nomenclature

Symbol		S.I. Unit
C_p	Specific heat at constant pressure	[J/(kg K)]
k	Turbulent kinetic energy	
F	Magnitude of buoyancy force	[N/m^3]
$\mathbf{I}$	Identity tensor	
p	Pressure	[Pa]
$\mathbf{n}$	Normal unit vector	
$\mathbf{U} \equiv (u,v,w)$	Velocity vector	[m/s]
U	Magnitude of velocity vector	[m/s]
t	Time	[s]
T	Temperature	[K]

Greek symbols

δ_w	Wall offset	[m]
κ	Karman's constant	
ε	Dissipation rate of turbulent kinetic energy	
λ	Thermal conductivity	[W/(m K)]
μ	Dynamic viscosity	[Pa s]
ρ	Density	[kg/m^3]

Subscript

in	Inlet
out	Outlet
T	Turbulent
ext	External

6. References

1. Balocco C., Petrone G., Cammarata G. Assessing the effects of sliding doors on an operating theatre climate. Building Simulation, v.5, no.1, p.73-84 (2012)
2. Brohus H, Balling KD, Jeppesen D. Influence of movements on contaminant transport in an operating room. *Indoor Air*, 16: 356-372 (2006)
3. Dharan S, Pittet D Environmental controls in operating theatres. *Journal of Hospital Infection*, 51: 79-84 (2002).
4. Dong S, Tu G, Cao R, Yu Z Numerical Study on Effects of Door-Opening on Airflow

Patterns and Dynamic Cross-Contamination in an ISO Class 5 Operating Room. *Trans. Tianjin University*, 15: 210-215 (2009).
5. Halvonovà B, Melikov AK Performance of ‘‘ductless’’ personalized ventilation in conjunction with displacement ventilation: Impact of disturbances due to walking person(s). *Building and Environment*, 45: 427–436 (2010).
6. Ignat L, Pelletier D, Ilinca F A universal formulation of two-equation models for adaptive computation of turbulent flows. *Computer Methods in Applied Mechanics and Engineering*, 189: 1119–1139 (2000).
7. Launder BE, Spalding DB The Numerical Computation of Turbulent Flows. Computer Methods in Applied Mechanics and Engineering. *Computer Methods in Applied Mechanics and Engineering*, 3: 269-289 (1974).
8. Matzumoto H, Ohba Y The Influence of a Moving Object on Air Distribution in Displacement Ventilated Rooms, *Journal of Asian Architecture and Building Engineering*, 3: 71-75 (2004).
9. Melhado MA, Hensen JLM, Loomans M, Forejt L Review of operating room ventilation standards. In: Proceedings of the 17th Int. Air Conditioning and Ventilation Conference (STP, Society of Environmental Engineering 2006), Prague, Czech Republic (2006).
10. Menazadeh F, Manning AP Comparison of Operating Room ventilation systems in the protection of surgical site. *ASHRAE Transactions*, 108: 1-13 (2002).
11. Shih YC, Chiu CC, Wang O (Dynamic airflow simulation within an isolation room. *Building and Environment*, 42: 3194–3209 (2007).
12. Talon D, Schoenleber T, Bertrand X, Vichard P Performances of different types of airflow system in operating theatre. *Annales de Chirurgie* 131: 316-321 (2006).
13. Wilcox DC Turbulence Modelling for CFD, DCW Industries Inc. (1998).

7. Acknowledgements

This work has been developed in collaboration with BE CAE & TEST (www.be-caetest.it) that is a COMSOL Certified Consultant.